Optical filter characterization by using optical frequency sweep technique with a single sideband modulator

Tetsuya Kawanishi[a)], Takahide Sakamoto, and Masayuki Izutsu

National Institute of Information and Communications Technology

4–2–1 Nukui-kitamachi, Koganei-shi, Tokyo 184–8795, Japan

a) *kawanish@nict.go.jp*

Abstract: We demonstrated optical filter characterization using optical frequency sweep with optical single sideband modulation technique, where the frequency shift range was 2 GHz–10 GHz. Undesired sidebands generated in the single sideband modulation due to electric phase errors can be compensated by automatic synchronized bias control. Fine pass band structures of a dual-section FBG were precisely measured, where the bandwidths of the pass bands were 440 MHz.
Keywords: optical frequency, optical modulation, single-sideband
Classification: Photonics devices, circuits, and systems

References

[1] T. Kawanishi and M. Izutsu, "Linear single-sideband modulation for high-SNR wavelength conversion," *IEEE Photon. Technol. Lett.*, vol. 16, pp. 1534–1536, 2004.

[2] M. Izutsu, S. Shikamura, and T. Sueta, "Integrated optical SSB modulator/frequency shifter," *IEEE J. Quantum Electron.*, vol. 17, pp. 2225–2227, 1981.

[3] S. J. Choi, Z. Peng, Q. Yang, E. H. Hwang, and P. D. Dapkus, "A semiconductor tunable laser using a wavelength selective reflector based on ring resonators," *OFC 2005*, PDP20.

[4] T. Kawanishi, Y. Matsuo, and M. Izutsu, "Suppression of undesired optical harmonics in wavelength conversion using optical single-sideband modulator," *CPT 2003*, D-13.

[5] S. Shimotsu, M. Izutsu, T. Kawanishi, S. Oikawa, and M. Sasaki, Wideband frequency conversion with LiNbO$_3$ optical single-sideband modulator, *OFC 2001*, WK3-1.

1 Introduction

Recently, we reported optical frequency conversion by using an optical single-sideband (SSB) modulator consisting of two Mach-Zehnder modulators [1, 2].

The frequency of the output lightwave depends on rf-signal frequency and dc-bias voltage fed to the modulator, which can be electronically controlled. Thus, by sweeping the rf-signal frequency, we can obtain an optical frequency sweeper whose output frequency can be swept agilely. Tunable lasers are often used for optical frequency sweep [3], but the relation between the output optical frequency and the electric signal for direct modulation or tuning of the laser can not described by a simple function. In addition, we should also handle mode hopping of lasers and frequency aberration due to fluctuation in temperature or injection current. On the other hand, in the optical frequency sweep by SSB modulators, the frequency shift from optical input is precisely equal to the rf-signal frequency. This is suitable for precise measurement of optical components and sensing technologies. However, the output lightwave contains undesired components due to imperfection of the modulator and the electric signal feeding circuits, which decreases the signal-to-noise ratio (SNR) of the output. In addition, optical harmonic generation in phase modulations also causes a drop of the SNR, and gives the theoretical limit of the SNR in the frequency conversion using an SSB modulator [3]. The phase errors in the electric signals, which cause generation of undesired sideband, can be compensated by optical phase delay which can be controlled by tuning dc-bias voltage applied to the modulator [4]. In this paper, we investigated optical frequency sweeper using SSB modulation with dc-bias voltage control, in order to obtain high-SNR wide frequency range sweep. We also demonstrated a measurement of fine structures in a reflection band of an optical filter.

2 Optical frequency shift with SSB modulator

The SSB modulator consists of a pair of Mach-Zehnder (MZ) structures as shown in Fig. 1 (a) [1, 2]. When we apply a pair of rf-signals, which are of the same frequency (f_m) and have 90° phase difference, to the electrodes RF_A and RF_B, frequency shifted lightwave can be generated at the output port of the modulator. Each sub MZ structure should be in null-bias point (lightwave signals in the paths have 180° phase difference), where the dc-bias can be controlled by DC_A and DC_B. To eliminate upper sideband (USB) or lower sideband (LSB), the lightwave signal in each path also should have 90° phase difference each other. When the phase difference induced by DC_C is 90°, we can get carrier-suppressed single sideband modulation comprising one of the sideband components (USB or LSB). The optical input should be a single-tone continuous lightwave. The output optical frequency is $f_0 + f_m$ or $f_0 - f_m$, where f_0 is the input optical frequency. Thus, we can control the output frequency by changing the rf-frequency f_m.

3 Optical frequency sweep for characterization of optical filters

Fig. 1 (b) shows our experimental setup for optical frequency sweep. A pair of rf-signals were fed to the electrodes RF_A and RF_B, via a 90-degree hybrid coupler. Optimal bias condition for high SNR optical frequency shift depends
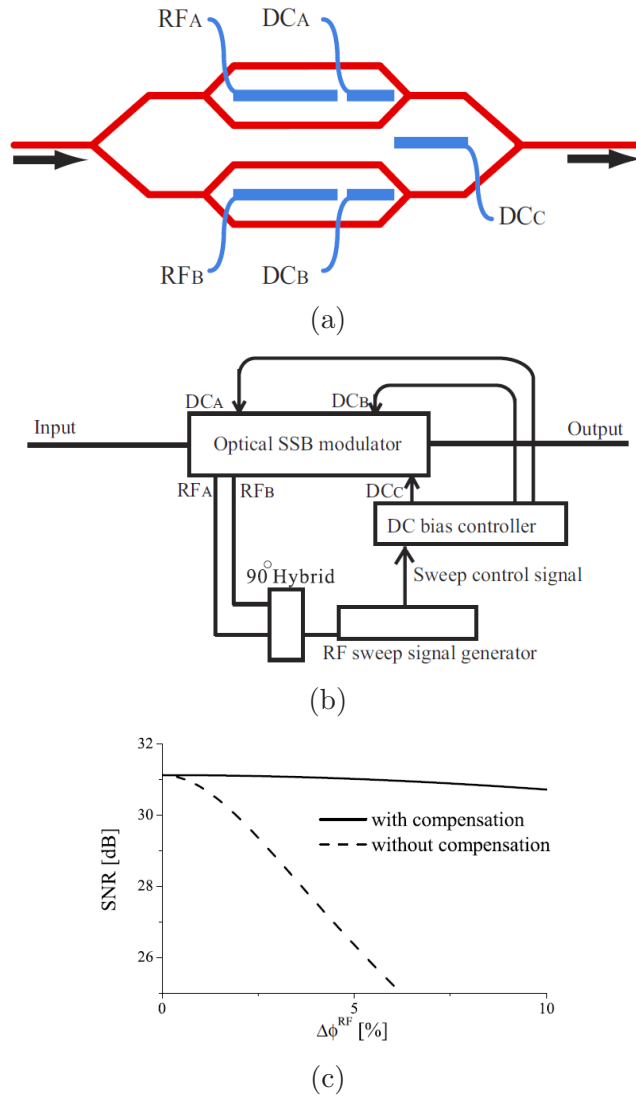
(a)

(b)

(c)

Fig. 1. (a) Schematic structure of SSB modulator. (b) Setup for optical frequency sweep. (c) Numerically calculated signal-to-noise-ratio (SNR) of modulator output with and without electric signal phase error compensation, where optical induced phase at each phase modulator in the SSB modulator was 0.8 rad. X-axis shows the electrical phase error $\Delta\phi^{\mathrm{RF}}$.

on the rf-frequency f_{m}. The suppression ratio of undesired components would be fluctuated during the frequency sweep operation. Thus, there is a trade-off relation between the suppression ratio and the sweep frequency range width. We used a dc-bias controller which can be synchronized with the frequency of the rf-signal sweeper, in order to obtain wideband optical frequency sweep without losing high suppression ratio. The phase errors in the rf-signal $\Delta\phi^{\mathrm{RF}}$ due to the hybrid coupler are dominant in generation of undesired spectra components. However, the phase error $\Delta\phi^{\mathrm{RF}}$ can be compensated by optical phase difference between the upper and lower arm in the modulator. Fig. 1 (c) shows the SNRs as functions of $\Delta\phi^{\mathrm{RF}}$. We get high SNR even when $\Delta\phi^{\mathrm{RF}}$
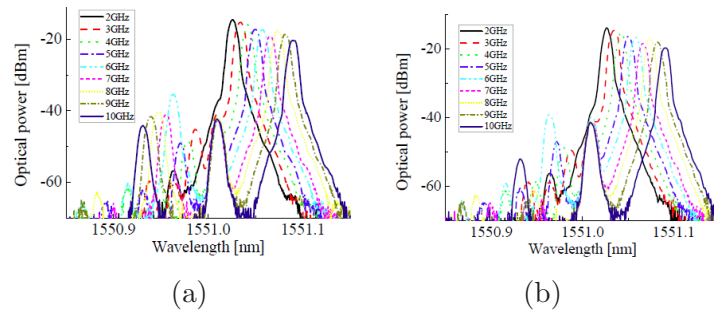
Fig. 2. (a) Optical output with a fixed bias condition.
(b) Optical output with synchronized bias control.

is large, by using the compensation of the phase error with the optical phase difference. For numerical calculation, we assumed that the amplitudes of rf-signals and lightwaves are balanced, and that the induced optical phase at each phase modulator due to the rf-signal is equal to 0.8 rad. We can control the optical phase difference by using dc-bias ports. The phase error at the hybrid can be compensated easily and agilely by tuning dc-voltage sources. The dc-bias controller has a table of optimal bias conditions as a function of the frequency, and can calculate continuously the three bias voltages DC_A, DC_B and DC_C according to the frequency control signal from the rf-signal sweeper. The rf-frequency was swept in 2–10 GHz. Fig. 2 (a) shows spectra of optical output without synchronization between the bias controller and the rf-signal sweeper where the bias voltages were fixed at the optimal condition for $f_m = 2$ GHz. The desired component (LSB) whose optical frequency was $f_0 - f_m$, was successfully generated, while there residual carrier and USB components. The intensity of LSB decreased as increasing the frequency. This is mainly due to frequency responses of travelling-wave electrodes of the modulator and that of the rf-signal feeding setup. As shown in Fig. 2 (b), the USB component was suppressed by using automatic synchronized bias control. The suppression ratio at 10 GHz frequency shift was 33 dB, while that without synchronized control was 24 dB. We generated continuous optical frequency sweep by using analogue ramp sweep from 3 GHz to 5.5 GHz. The sweep time was 10 ms, which was limited by the rf-signal sweeper. Fine structures in the reflection band of a dual-section fibre Bragg grating (FBG) were measured by using the optical frequency sweep signal. The transmittance can be obtained from the optical power in time domain, where the data should be compensated by a reference signal measured out of the reflection band of the FBG. For comparison, the transmittance of the FBG was also measured by a tuneable laser is shown in Fig. 3 (a). There were a series of narrow pass bands in the reflection band. The pass bands at the points A, B and C indicated in Fig. 3 (a) consisted of sub two peaks whose separation was 1.2 GHz. We measured the fine structures near the points A, B and C by feeding the optical sweep signal to the FBG. As shown in Fig. 3 (b), the frequency separations between a pair of peaks were 1.2 GHz, which agreed with the result in Fig. 3 (a). The 3-dB bandwidth of the larger peak at the point B was 440 MHz. The SSB modulator was constructed on an x-cut LiNbO₃
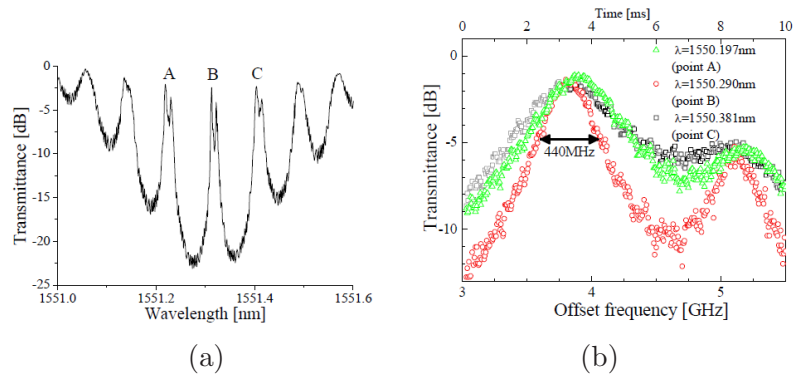
Fig. 3. (a) Transmittance of a dual-section FBG measured by a tuneable laser. (b) Fine structure of transmittance measured by optical frequency sweep.

substrate, so that the electric field of the lightwave in the modulator should be horizontally polarized with respect to the substrate surface, where the polarization state of the lightwave at the FBG can be controlled by using a polarization controller.

4 Conclusions

We demonstrated high-speed optical frequency sweep using SSB modulation technique, where the sweep range was 2 GHz to 10 GHz. Fine pass band structures of a dual-section FBG were precisely measured, by the optical frequency sweep signal.

Acknowledgments